J. Korean Asso. Radiat. Prot.
Vol. 23, No. 1 : (1998)

■ 論 文 ■

Establishment of the Monoenergetic Fluorescent X-ray Radiation Fields

Jang-Lyul Kim, Bong-Hwan Kim, Si-Young Chang and Jae-Ki Lee*
Korea Atomic Energy Research Institute
*Han-Yang University**

교정용 단일에너지 형광 X-선장의 제작

김장렬 · 김봉환 · 장시영 · 이재기*
한국원자력연구소, *한양대학교

Abstract - Using a combination of an X-ray generator installed in radiation calibration laboratory of Korea Atomic Energy Research Institute (KAERI) and a series of 8 radiators and filters described in ISO-4037, monoenergetic fluorescent X-rays from 8.6 keV to 75 keV were produced. This fluorescent X-rays generated by primary X-rays from radiator were discriminated K_β lines with the aid of filter material and the only K_α X-rays were analyzed with the high purity Ge detector and portable MCA. The air kerma rates were measured with the 35 cc ionization chamber and compared with the calculational results, and the beam uniformity and the scattered effects of radiation fields were also measured.

The beam purities were more than 90 % for the energy range of 8.6 keV to 75 keV and the air kerma rates were from 1.91 mGy/h (radiator : Au, filter : W) to 54.2 mGy (radiator : Mo, filter : Zr) at 43 cm from center of the radiator. The effective area of beam at the measurement point of air kerma rates was 12 cm X 12 cm and the influence of scattered radiation was less than 3 %. The fluorescent X-rays established in this study could be used for the determination of energy response of the radiation measurement devices and the personal dosemeters in low photon energy regions.

Keywords : fluorescent X-rays, beam purities, air kerma rates, radiator and filter

요약 - 한국원자력연구소 교정시설에 설치되어 있는 MG325 X-선 발생장치와 ISO-4037에서 제시하고 있는 라디에이터 및 필터 8종을 조합하여 8.6 keV 부터 75 keV 까지의 단일에너지 형광 X-선을 제작하였다. 1차 X-선에 의하여 라디에이터에서 발생된 형광 X-선중 K_β를 필터를 사용하여 제거한 후 단지 K_α만의 형광 X-선 스펙트럼을 고순도 평판형 반도체검출기와 휴대용 다중파고분석기로 분석하였으며 35 cc 전리함을 이용하여 이때의 선량률 (air kerma rates)를 측정하여 계산결과와 비교하였다. 또한 방사선장의 균일도분포를 전리함과 사진현상을 통하여 결정하였으며 산란 X-선의 영향도 측정하여 실제

적용가능성을 검토하였다.

실험결과 순도가 90 % 이상되는 8.6 keV부터 75 keV까지의 단일에너지 형광 X-선을 얻었으며 라디에이터 중심으로부터 43 cm 위치에서의 선량률은 1.91 mGy/h (라디에이터 : Au, 필터 :W)로부터 54.2mGy(라디에이터 : Mo, 필터 : Zr) 까지였다. 선량률 측정지점에서 방사선장의 유효면적은 12 cm X 12 cm로 계측기의 교정이나 개인선량계의 조사에 전혀 문제가 없음을 확인하였고 산란방사선의 영향도 3% 이하였다.

중심단어 : 형광 X-선, 순도, air kerma rates, 라디에이터 및 필터

Introduction

The energy responses to the low energy photon (10~300 keV) for the radiation measurement devices such as surveymeter, TLD and film badge, etc are very different from those of the high energy photons (^{137}Cs, ^{60}Co). The characteristics test of the instruments for low energy photon range is usually performed by using the continuous X-ray spectra but the energy responses for that spectra are also different from those of the monoenergetic photons. Above the energy of 100 keV of the X-ray tube potential, the calculated dose conversion coefficients based on the continuous distribution of X-ray spectra have not big differences with those of spectrum average energy by interpolation of the values represented in the ICRU 47, ICRP Publication 51 and 74[1~3], but below 100 keV this difference can not be negligible and in this case the monochromatic radiations become useful for calibrating of instruments. It is clear the differences between these two values for ANSI N13.11[4] and ISO 4037[5] Narrow and Wide X-ray series in Table 1. We can see in this table that the larger the resolution of the spectrum, the bigger the difference of the values in the lower energy ranges.

There are a couple of different types of monoenergetic radiation sources such as gamma emitting, radionuclides that decay by electron capture or internal conversion to ground state and emit X-rays, and gamma sources that are used to cause fluorescence in a secondary target which then emits its characteristic X-rays. But radionuclides and gamma sources are very limited because there are only small number of such radionuclides with essentially monoenergetic emissions and their energy range is also restricted. Moreover it should be considered the half life of the radionuclide and self absorption in the source which is serious if the gamma ray or X-ray energy is low.

Another method to generate the monoenergetic radiations is to use the X-ray generator in conjuction with interchangable radiators and filters by which it is possible to get different types of monoenergetic X-rays ranging from ~ 10 keV to 100 keV. This system has a number of advantages over the radionuclides such that high kerma rates compared with the isotopic sources, various energy ranges with radiator materials, variable air kerma rates by adjusting the X-ray tube currents and convenience by shutoff the machine when not in use.

The system to generate monochromatic X-ray has been known for decades[5~15]. The purpose of this study, by applying the spectrum unfolding of measured spectra with the HPGe detector which was never used in the other literatures, is to produce K_α fluorescent X-rays and to evaluate spectrum purities, beam uniformity, scattered effects of the system and air kerma rates of 8 energies recommended in the ISO-4037. The established system at KAERI radiation calibration laboratory can offer the calibration services of the radiation measuring instruments and the energy response tests of the personal dosemeters with the monoenergetic

Table 1. Conversion coefficients for average energy and monoenergy of ANSI N13.11 and ISO Wide and Narrow X-ray fields.

E (keV)	Resolution (%)[1]	C.F.(Sv/Gy)		C.F.(Sv/Gy)[3]
		ANSI[2]	ISO[2]	
ANSI M30 (20)	74	0.42		0.613
M60 (35)	102	1.00		1.308
M100 (53)	93	1.52		1.820
M150 (73)	116	1.78		1.911
H150 (118)	39	1.71		1.731
ISO N40 (33)	30		1.17	1.228
N60 (48)	36		1.65	1.727
N80 (65)	32		1.88	1.911
N100 (83)	28		1.88	1.881
N120 (100)	27		1.81	1.812
N150 (118)	37		1.73	1.731
N200 (163)	30		1.57	1.561
N250 (205)	28		1.48	1.481
N300 (300)	27		1.42	1.424
ISO W60 (45)	48		1.55	1.651
W80 (57V)	55		1.77	1.867
W110 (79)	51		1.87	1.767
W150 (105)	56		1.77	1.790
W200 (137)	57		1.65	1.649
W250 (173)	56		1.54	1.537
W300 (208)	57		1.47	1.477

1) Data for resolutions of ANSI series from measurements at KAERI X-ray fields.
2) Data from Ref. 4 and 5.
3) The values are interpolated by monoenergy photons in ICRP 74.

photon radiations from ~ 10 keV (K_α of Zn) to 1,250 keV (^{60}Co) to the industry.

Fluorescent X-ray Generation

The production principle of the fluorescent X-rays is the conversion of the primary X-rays having continuous spectrum from the X-ray tube to the monoenergetic K_α X-ray beams by bombarding the radiator with the primary X-rays. When a X-ray photon that has a energy higher than the K shell absorption edge of the radiator interacts with an atom, one interaction involves the transfer of the photon energy to one of the K shell elements of the atom resulting in its ejection from the atom. The distribution of electrons returns to the normal state by transitions of electrons from outer shells to inner shells. The energy difference between these states is emitted as either a characteristic K X-ray or an Auger electron. But the K characteristic X-rays include not only K_α photon ejected from L electron to K shell but also K_β photon from M electron because of the continuous energy distribution of the primary X-ray beams. To obtain monoenergetic high purity K_α X-ray photons it is necessary to decrease the K_β X-rays by adding the secondary filter between radiator and measurement point. The optimum choice of the filter material for a radiator with atomic number Z is based on the concept that the filter material has a K absorption edge energy either slightly

higher than the energy of K_β line or between the K_α and K_β lines of the radiator. Thus it is general that the element of Z-1 ~ Z-5 of the radiator according to the K_α and K_β energies of the radiator is used for the filter material. Also the filter material can be either in a metal form or stable chemical form[5].

In this study 8 types of K fluorescent X-rays having energies between 8.6 keV to 75 keV as indicated in Table 2 according to the list of ISO-4037[5] were produced. The schematic diagram of system used for the experiment is in Fig. 1. The X-ray generator was a MG325 (Phillips, Germany) having a maximum potential up to 320 kV. The primary beams from the X-ray generator were collimated with a tungsten collimator to strike the radiator which was placed at a 45° angle and 60 cm from the X-ray tube target. The radiator had a dimension of 10 cm X 10 cm and fluorescent X-rays produced at the radiator emitted with the 90° degree to the primary X-rays through the filter to reduce the K_β fluorescent X-rays, then finally the energy spectra and air kerma rates of

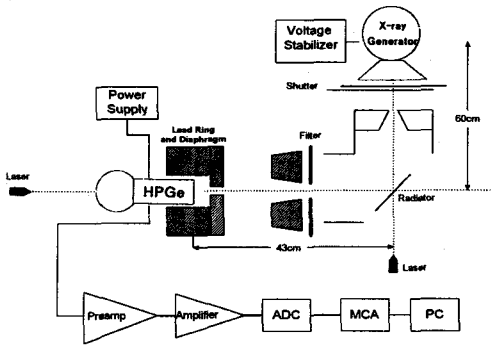

Fig. 1. Schematic diagram of system used to study the production of fluorescent X-rays.

K_α X-rays were measured at the distance of 43 cm from the radiator.

Theoretical Formulation for Fluorescent X-Rays

The first factor to be considered for a calculation is the incident flux, $N_0(E)$, of primary X-rays on the surface of the radiator with a small energy range between E and dE. This

Table 2. Radiators and filters used for fluorescent X-rays.

No.	Theore. energy K_α(keV)	Radiator		Tube potential (keV)	Primary filter (g/cm^2)	Secondary filter	
		Ele.	Mass(g/cm^2)			Ele.	Mass(g/cm^2)
8[1]	68.8	Au	0.6 (0.0122″)	170	Al 0.27	W	0.6 (0.0122″)
9	75.0	Pb	0.6 (0.0122″)	190	Al 0.27	Au	0.6 (0.0122″)
11	8.64	Zn	0.6 (0.0122″)	50	Al 0.135	Cu	0.6 (0.0122″)
12	17.5	Mo	0.6 (0.0122″)	80	Al 0.27	Zr	0.6 (0.0122″)
13	25.3	Sn	0.6 (0.0122″)	100	Al 0.27	Ag	0.6 (0.0122″)
14	37.4	Nd[2]	0.6 (0.0122″)	110	Al 0.27	Ce[2]	0.6 (0.0122″)
15	49.1	Er	0.6 (0.0122″)	120	Al 0.27	Gd	0.6 (0.0122″)
16	59.3	W	0.6 (0.0122″)	170	Al 0.27	Yb	0.6 (0.0122″)

[1] No. of ISO standard.
[2] These foils should be properly sealed to prevent oxidation.

primary X-ray spectra could be calculated by the methods described in different papers[16, 17]. Other factors are: (1) the decrease of the primary X-ray intensities reaching a layer of thickness dx at a depth of x in the radiator, (2) the decrease of the fluorescent X-ray intensities which have to pass through a depth of x to escape the radiator, (3) the incident angle, ϕ, of the primary X-ray and the fluor-escent X-ray escape angle, θ (See Fig. 2).

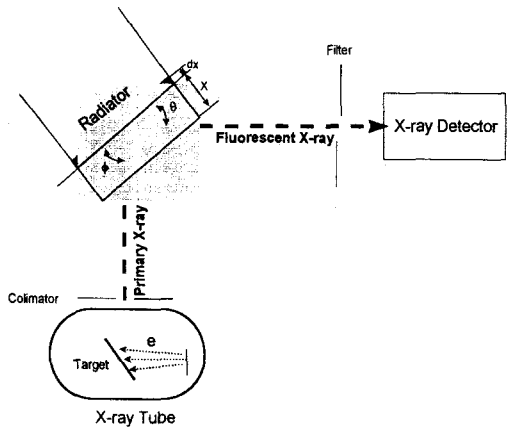

Fig. 2. Illustration of the fluorescent X-rays for theoretical calculation.

As illustrated in Fig. 2, the number of X-rays, N(E)dE, at a depth x is

$$N(E,x)dE = N_0(E)dE \cdot \exp(-\mu(E)x/\sin\phi) \quad (1)$$

where $\mu(E)$ is the linear absorption coefficient for X-ray energy E. When the primary X-rays pass through the layer of radiator dx, the number of X-rays absorbed is

$$dN(E,x) = N(E,x)dE \cdot (1-\exp(-\mu(E)dx/\sin\phi)). \quad (2)$$

Where $dx \rightarrow 0$, then

$$dN(E,x) = N(E,x)dE \cdot \mu(E)dx/\sin\phi. \quad (3)$$

So these X-rays are contributed to the emission of fluorescent K X-rays. The emission probability of fluorescent K_α X-rays, R, is

$$R = f \cdot \omega \cdot P_\alpha \quad (4)$$

where f is the correction factor for only K absorption to all the electron energy levels absorption, ω is K shell fluorescent yield and P_α is the production probability of K_α. Only the K absorption is to be considered, the correction factor f can be expressed as

$$f = \mu_K(E)/\mu_T(E) = (S_K-1)/S_K \quad (5)$$

where $\mu_K(E)$ and $\mu_T(E)$ are the K and total linear absorption coefficients at energy E, and S_K is the K absorption jump ratio. The ω is the ratio of K X-rays to the total number of de-excitations to the K shell. And it is only considered the production of K_α X-rays, the probability P_α of a K_α is included in Eq. (4).

Therefore the number of K_α X-rays produced at the layer of dx is

$$dN_{K\alpha}(E,x) = R \cdot dN(E,x). \quad (6)$$

From Eq. (1), (3) and (6)

$$\begin{aligned} dN_{K\alpha}(E,x) &= R \cdot N(E,x)dE \cdot \mu(E)dx/\sin\phi \\ &= [R \cdot \mu(E)dx \cdot N_0(E) \cdot \exp(-\mu(E)x \\ &\quad /\sin\phi)] / \sin\phi. \end{aligned} \quad (7)$$

The fluorescent X-rays produced at the layer of dx are decreased by the radiator which has the depth of x and the angle of exit θ. The probability to arrive at the radiator surface is

$$\exp(-\mu(E_\alpha) \cdot x/\sin\theta) \quad (8)$$

where $\mu(E_\alpha)$ is the linear absorption coefficient at the energy of the K_α X-ray, $E_{K\alpha}$. So the number of K_α emitted at the surface of radiator

has to integrate both over x and the range of primary X-ray energy from the K absorption edge (E_K) to the maximum energy (E_0),

$$N_{K\alpha} = \frac{R}{\sin\phi}\int_{E_K}^{E_0}\mu(E)N_0 dE\int_0^X \exp(-x(\mu(E)/\sin\phi+\mu(E_\alpha)/\sin\theta))dx \quad (9)$$

where X is the radiator thickness. If X is very large compared to the penetration depth of the X-rays, then Eq. (9) reduces to

$$N_{K\alpha} = \frac{R}{\sin\phi}\int_{E_K}^{E_0}\frac{\mu(E)N_0 dE}{(\mu(E)/\sin\phi)+(\mu(E_\alpha)/\sin\theta)} \quad (10)$$

If the area of radiator to be irradiated from primary X-ray is S (cm^2), the linear absorption coefficient and the thickness of the secondary filter are μ_a (cm^{-1}) and t_f (cm) respectively, and the distance from the center of radiator to the measurement point is L (cm), then the number of $K_{\alpha 1}$ X-rays per unit area at the measurement point, $N_{\alpha 1}$, is

$$N_{\alpha 1} = \frac{R}{\sin\phi}\cdot\exp(-\mu_a(E_{\alpha_1})\cdot t_f/\sin\phi)\cdot\frac{S}{4\pi L^2}\cdot\int_{E_K}^{E_0}\frac{\mu(E)N_0 dE}{(\mu(E)/\sin\phi)+(\mu(E_{\alpha_1})/\sin\theta)} \quad (11)$$

Like above method it can be calculated the number of $K_{\alpha 2}$ and K_β separately, but our concern is focussed at the $K_{\alpha 1}$ in the high purity fluorescent X-ray fields, so only the $K_{\alpha 1}$ is calculated. After calculations of the number of $N_{\alpha 1}$ for the 8 fluorescent energies, they are converted to air kerma rates (K_a) using the data of air kerma in free air to fluence in ICRU 47[1], and compared them with the experimental results.

Experiments

Energy Spectra of the Fluorescent X-rays

The K X-rays emitted from the radiator were measured with the planar type high pur-ity semiconductor detector (HPGe, GLP32340-p, Ortec) and the portable multichannel analyzer (PMCA-7500B, Ortec). Schematic diagram is illustrated in Fig. 1. The entrance window surface of the HPGe detector was placed at 43 cm from center of the radiator which was the just same position with the measurement of air kerma rates. The detector was shielded by 1 cm thickness lead with a 0.8 mm diameter hole at the center of lead against saturation of the detector. The high voltages and currents of the X-ray generator were the actual conditions for the measurement of air kerma rates. Prior to the measurement, channel-energy calibration of the detecting system was carried out with the known energies standard gamma sources of Ba-133, Am-241 and X-rays of Cs-137.

Purities of the fluorescent X-rays

The purities of the fluorescent X-rays were evaluated by calculation from the spectrum measured at previous section. The spectra were measured with several tube potentials to determine the optimum high voltage to have the high spectral purity. Then each spectrum was divided into 0.5 keV energy interval and unfolded it for correction of K-escape fraction, Compton continuum and the detection efficiency of the HPGe detector. The detection efficiency and the unfolding method for our system were described in other articles[18, 19] in detail.

After correcting the spectrum a purity defined as the number of K_α counts to the numerical integration of the total counts from the HPGe detector was calculated. From the calculation results high voltage at which the purity was more than 90 % was selected as the operation voltage for calibration uses.

Beam Uniformity

The fluorescent X-ray source produced by the radiator has the form of an ellipse oriented at 4

5° to the primary X-ray beams. Moreover, this source is inhomogeneous since the flux of primary photons causing interactions followed by the emission of fluorescent X-ray is not constant throughout the irradiated surface of the radiator. This is because each surface element of the radiator is at a variable distance from the focal spot of the X-ray tube. Therefore the homogeneity of radiation field at the measurement point of fluorescent X-rays should be considered for calibrating a large size of chamber or irradiating a number of personal dosemeters simultaneously. Theoretical calculation of the homogeneity problems was already performed by Chartier et al.[20], so in this work the experimental measurements were only done by the methods of photographic film densitometry and ionization chamber dosimetry.

For chamber dosimetry, NE2530/1 35cc ionization chamber and Victoreen 530 electrometer were used. This chamber was calibrated for the fluorescent X-rays at secondary standard laboratory of the Institute of Radiation Protection and Safety (IPSN/CEA) in France by Mesh Grid Type IIc free ionization chamber. It was also used for measuring of scattered radiation and air kerma rates in next sections. For uniformity measurement, radiator and filter material were Mo and Zr (17.5 keV, see Table 2.) , and high voltage and current were 80 kVp and 10 mA, respectively. The ionization chamber was placed in a plane of vertical and horizontal to the center of the fluorescent X-rays (43 cm from radiator) with the two consecutive points distance of 1 cm. Then the air kerma rates were normalized to 1 at the center of beam.

For densitometry by photographic film, Kodak X-Omat V film for therapy verification made in Eastman Kodak Company, USA was irradiated at the center of fluorescent X-rays. But the film was attached on a PMMA phantom which had a dimension of 30 cm X 30 cm X 15 cm because the personal dosemeters would be irradiated on the phantom. After developed the film it was read the densities by a fully automatic densitometer (Model 1705 Film Dens-itometer, Germany) installed in Yonsei Medical Center. The densities were also normalized to 1 at the center of beam.

Scattered Radiation

ISO 4037 recommended that the contribution due to scattered radiation should be checked at the experimental distance to measure the air kerma rates. If this contribution is more than 5% of the total air kerma rate, the effectiveness of the X-ray shielding must be checked again. This test was carried out with the aid of a same dosimetry system of above section. The fluorescent X-rays were 17.5 keV (radiator : Mo, filter : Zr, H.V. : 80 kVp, current : 20 mA) which was the highest air kerma rate and 75 keV (radiator : Pb, filter : Au, H.V. : 190 kVp, current : 10 mA) which had the highest energy of our system. The air kerma rates were measured on the central axis of the beam at the various points of distance. These rates, after correction for air attenuation and for inverse square of the focus to detector distance with distances, were checked to have a proportionality within 5%.

Air Kerma Rates of Fluorescent X-Rays

NE 2530/1 ionization chamber described at the previous section was used for the measurement of air kerma rates from the fluorescent X-rays. The calibration results are in Table 3 for the ISO 4037 fluorescent X-ray series. The distance for measuring the air kerma rates was 43 cm from the center of the radiator. Having corrected by temperature and pressure, the electrical charge produced in ionization chamber were converted to air kerma rate by multiplying the calibration factors in Table 3. To obtain various air kerma rates, two kinds of currents of the X-ray tube were selected at each applied high voltage. Measured data were compared to the calculation results described in the calculation section.

Table 3. Calibration factors for fluorescent radiations calibrated at IPSN/CEA.

Radiation quality	Energy (keV)	Air Kermarate ($Gy \cdot h^{-1}$)	Current (pA)	Calibration factor ($Gy \cdot h^{-1} \cdot A^{-1}$)	Uncertainty (%)
F-Ge	9.9	1.0049E-01	19.6490	5.1140E+09	2.60
F-Zr	15.8	8.7229E-02	26.2730	3.3201E+09	2.60
F-Cd	23.2	7.2760E-02	23.7500	3.0630E+09	2.60
F-Cs	31.0	4.4105E-02	14.4010	3.0630E+09	2.60
F-Sm	40.1	3.7816E-02	12.3930	3.0500E+09	2.60
F-Er	49.1	4.5720E-02	14.7710	3.0950E+09	2.60
F-W	59.3	2.2888E-02	7.4897	3.0560E+09	2.60
F-Pb	75.0	9.0947E-03	2.9600	3.0730E+09	2.60

Results and Discussion

Energy Spectra of the Fluorescent X-rays

Usually three factors prevent the fluorescent X-ray from being truly monoenergetic. First, there are four significant K X-rays resulted from a vacancy in the K shell from a photoelectric interaction. Namely, $K_{\alpha 1}$ and $K_{\alpha 2}$ are transitions from $L_{III} \rightarrow K$ and $L_{II} \rightarrow K$, and $K_{\beta 1}$ and $K_{\beta 2}$ are from $M \rightarrow K$ and $N \rightarrow K$, respectively. K_β lines can be eliminated from the spectra by aid of the secondary filter, but in high K_β energy these lines could be a little important portion. Second, in high atomic number element the L X-rays (transitions from higher shells down to the L shell) have sufficient energy to become apparent; and third, scatter from distribution of X-ray energies of the primary beam, but this problem can be solved by proper shielding of the fluorescent X-ray generating system.

Fig. 3 shows the measured fluorescent X-ray spectra. As seen in the Fig. 3, all of the spectra have sharp peak for a K_α fluorescent X-ray and K_β lines are nearly discriminated by the secondary filter. The smaller peaks about 10 keV below the K_α in low energy X-ray regions are due to the loss from the detector of Ge X-ray (X-ray escape peak), and a little K_β lines and scattering radiations are remained in the higher energy regions more than 170 kVp. Also the small peaks just below K_α X-rays are due to the photoelectric absorption of the detector. The L X-rays of 75 keV (Pb radiator) are seen to be a little prominent in the spectrum. But X-ray escape peak, photoelectric absorption peak, Compton continuum and pile up of the all of the spectra were removed as minimum by unfolding the measured spectra, and these spectra can be used satisfactorily as the monochromatic radiations.

Purities of the fluorescent X-rays

The optimum X-ray tube potential for maximum purity of the fluorescent X-rays is approximately twice the K absorption edge energy for the relevant radiator[5]. If the higher air kerma rates are required it is possible to use higher values of tube potentials, but this will result in a lower purity of the radiation. Fig. 4 shows the spectrum purities with the applied tube potentials. The spectral purities were calculated by numerical integration of the (K_α) or (K_α + K_β)/(Total Intensity) from the spectral distributions of the unfolded spectra mentioned previous section. From these results we can see

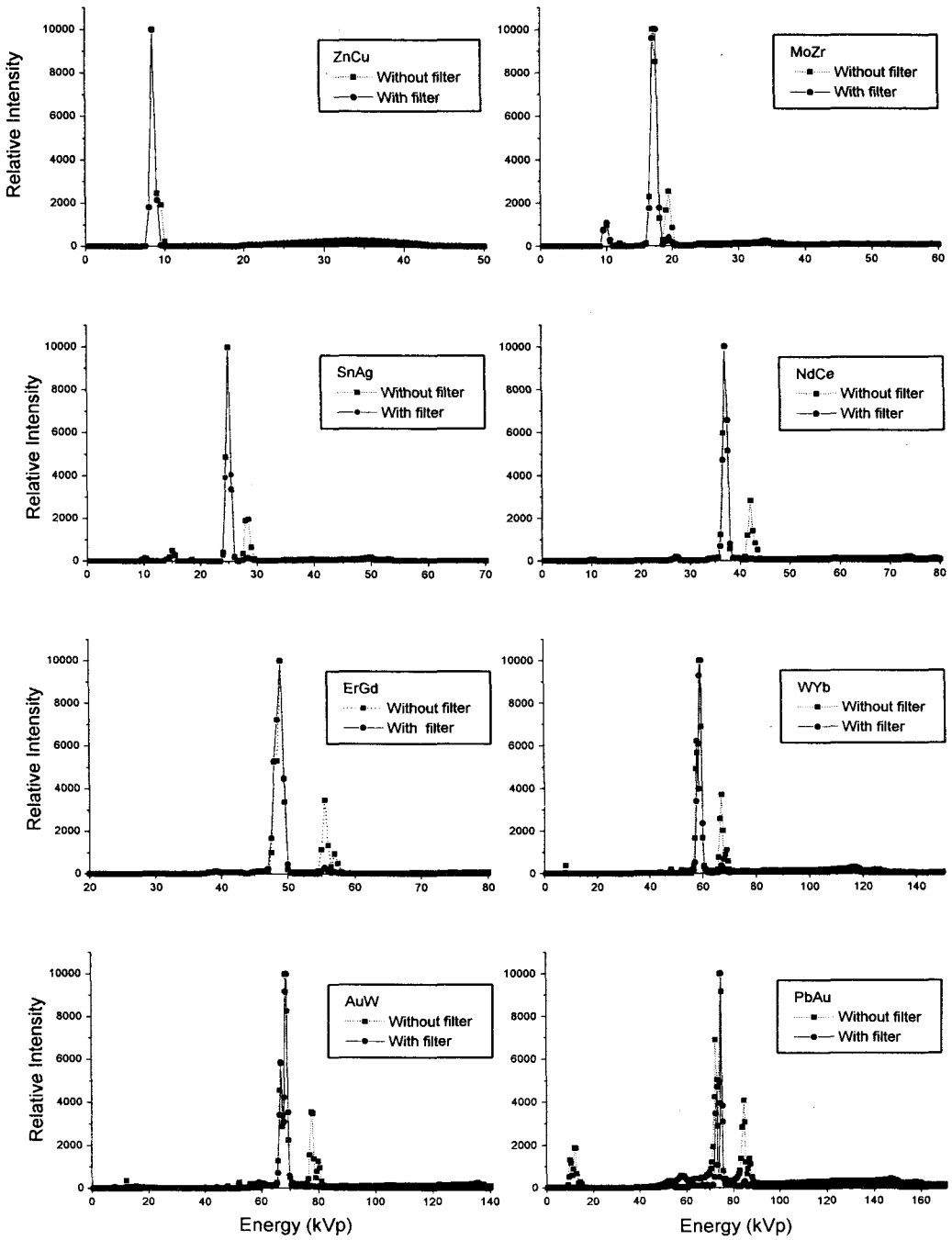

Fig. 3. Measured fluorescent X-ray spectra. In legend, left material is radiator and right one is target.(For example, Zn is radiator and Cu is filter in ZnCu.)

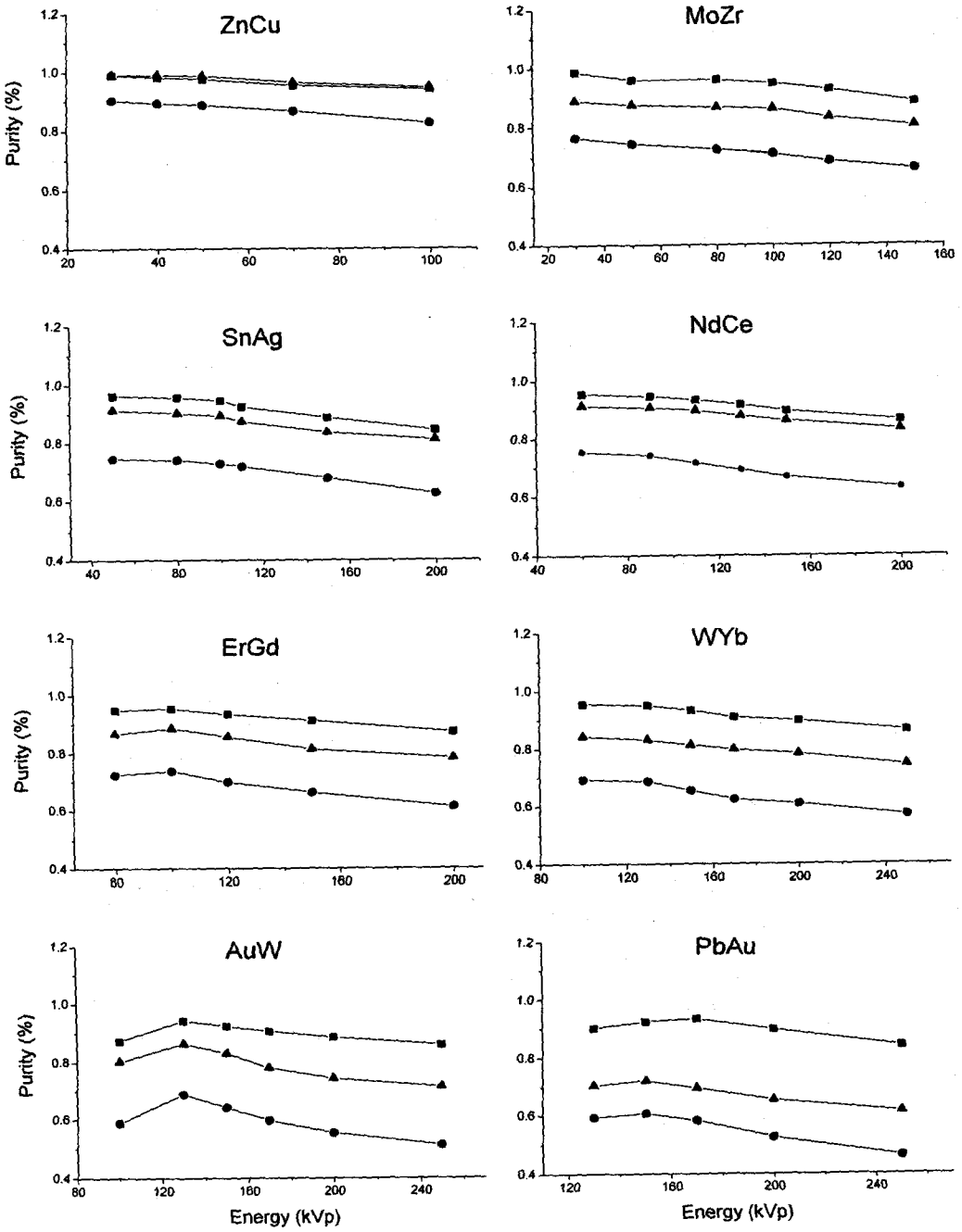

Fig. 4. Fluorescent X-ray purities as a function of X-ray tube potential. (■ : with filter, ▲ : without filter(K_α+K_β) and ● : without filter(K_α only))

Table 4. Purities of fluorescent X-rays for selected tube potential.

Radiator	Filter	$E_{K\alpha}$ (keV)	H.V. (kVp)	Current (mA)	Purity (%)		
					With Filter	Without Filter	
						K_α only	$K_\alpha+K_\beta$
Zn	Cu	8.6	50	20	0.975	0.886	0.989
Mo	Zr	17.5	80	20	0.960	0.724	0.866
Sn	Ag	25.3	100	10	0.945	0.728	0.892
Nd	Ce	37.4	110	10	0.932	0.715	0.896
Er	Gd	49.1	120	10	0.934	0.699	0.854
W	Yb	59.3	170	10	0.908	0.624	0.796
Au	W	68.8	170	10	0.905	0.598	0.778
Pb	Au	75.0	200	10	0.897	0.525	0.652

the purities of the fluorescent X-rays are decreased with the increasing applied tube potentials. When the radiator was Er, the purities were expected to more decrease than other radiators because it was a chemical form of Er_2O_3 not a metal form, but it did not exist low purities compared to the others. Particular high purities were obtained in the low energy fluorescent X-rays of radiator Zn and Mo because the air absorption coefficients of air is large for low energy photons from which they are largely absorbed by the air.

Even though it was difficult to match the recommended X-ray tube potentials of ISO 4037 because of a little low purities in high energy regions of Au and Pb, it could be obtained spectral purities more than 90 % in the optimal range of tube potentials for each particular radiator. The results of the purity measurements for selected tube potential are summarized in Table 4. The spectral purities were also plotted in Fig. 5 as a function of X-ray tube currents at determined potential for the purpose of determining the several air kerma rates in which the severe variations of spectral purities were not observed.

Beam Uniformity

Fig. 6 shows the air kerma rates curve as a function of distance in the direction of X- and Y- axis respectively, moved from the center of the plane where the ionization chamber is located, namely the plane of the distance of 43 cm from the center of radiator (16 cm from the

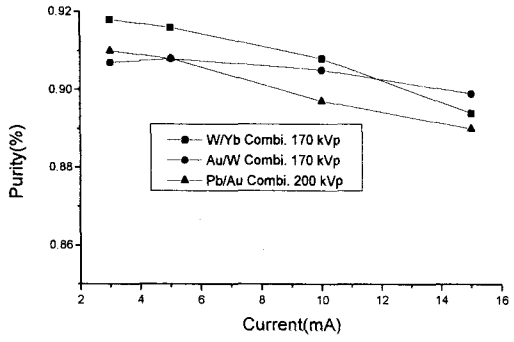

Fig. 5. Spectral purities with the X-ray generator tube currents.

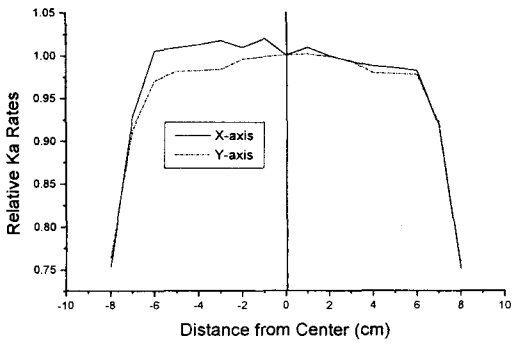

Fig. 6. Beam homogeneity curves of fluorescent X-ray by ionization chamber. (Radiator : Mo, Filter : Zr, 80 kVp, 10 mA.)

Fig. 7. Homogeneity lines of the Fluorescent X-rays by densitometry. Homogeneity are 95%, 90%, 70%, 60%, 50% from inside to outside.

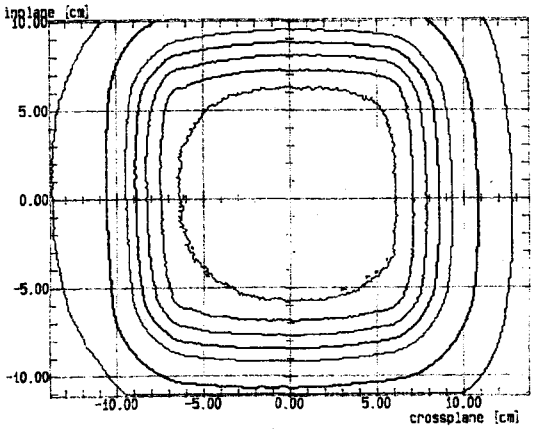

secondary filter material having dimension of 10 cm X 10 cm). Consecutive measuring distance interval was 1 cm and normalized the air kerma rates to that of center. In Fig. 6 the air kerma rates were not corrected for the distance differences between the center of the plane and the X- and Y- axis measurement points. A little contribution of scattered radiations could be seen in the direction of negative X- axis, but the diameter of radiation fields in which the beam uniformity had more than 97 % was about 12 cm.

Because beam uniformity data by the ionization chamber dosimetry was obtained only for the X- and Y- axis to the center of the radiation field, the remaining parts in plane were checked by film densitometry. The result is shown in Fig. 7 and the beam uniformity was nearly same as the dosimetry method.

In ISO 4037 it is recommended that the variation in air kerma rates of the fluorescentX-ray beam over the area of the detector employed should not be greater than 5 %, and the beam cross section at the point of irradiation should always be greater than the cross sectional area of the instrument being calibrated. From our experimental results, the beam uniformity more than 97 % in the fluorescent X-ray of diameter 12 cm was obtained and it could be used for not only the calibration of general surveymeter but also the simultaneous irradiation of four personal dosemeters.

Table 5. The results of air kerma rate measurements with the distances.

Distance	K_a Rate (mGy/h)	Relative K_a at Initial distance
Radiator : Mo, Target : Zr, 80 kVp, 20 mA		
Initial Distance (43cm from Center of Target)	54.52	1
Initial Distance + 10 cm	35.3271	0.998
Initial Distance + 20 cm	24.3835	0.987
Initial Distance + 30 cm	17.8485	0.983
Initial Distance + 40 cm	13.5476	0.978
Initial Distance + 50 cm	10.6274	0.977
Initial Distance + 60 cm	8.5928	0.982
Radiator : Pb, Target : Au, 190 kVp, 10 mA		
Initial Distance (43cm from Center of Target)	4.5707	1
Initial Distance + 10 cm	3.0241	1.007
Initial Distance + 20 cm	2.1449	1.012
Initial Distance + 30 cm	1.6015	1.016
Initial Distance + 40 cm	1.2395	1.019
Initial Distance + 50 cm	0.9877	1.022
Initial Distance + 60 cm	0.8071	1.026

Scattered Radiations

The air kerma rates on the central axis of the fluorescent X-ray beams at the points of 10 cm interval are in Table 5. Also the values corrected by distances and air attenuation are in the same Table. No significant scattered radiations were observed in 17.5 keV K X-rays at which the air kerma rates were conversely decreased by small amounts for the low energy photon absorption in air. A little scattering radiations were found out at the 75 keV high energy K X-rays but the portions were less than 3%.

Air Kerma Rates of Fluorescent X-Rays

The air kerma rates of each fluorescent X-ray were measured at the distance of 43 cm from the center of the radiator, and the results are in Table 6 with the calculation results discussed in previous section. Because the spectrum purities were not varied with the currents as shown in purity measurement section and the air kerma rates would be sometimes needed to change with the calibrations or irradiations of dosemeters, the air kerma rates were measured at two different currents. The calculation results were always lower than those of the experiment because the K_β lines, scattered radiations and other factors to be affected to the measurement results were not considered in calculation.

Maximum air kerma rate was 54.52 mGy/h in case of Mo radiator and Ag filter. Even though Au radiator and W filter had the lowest air kerma rates (1.91 mGy/h) all of the fluorescent X-rays could be satisfactorily used for the calibration activities in secondary standard laboratory.

Conclusions

For the purpose of using monochromatic low energy photon radiations useful in the calibration of instruments or in the irradiation of personal dosemeters with the energies, K fluorescent X-ray beams ranging from 8.6 keV to 75 keV were produced. The spectral puriries for the 8 radiators were more than 90%, it means that only the K_α X-rays were emitted. Also the beam uniformity was sufficiently large to irradiate or calibrate the dosemeters and scatter-

Table 6. Air kerma rates by measurement and calculation produced in this study.

Target	Filter	$E_{k\alpha}$ (keV)	H.V. (kVp)	Current (mA)	K_a by Measurement (mGy/h)	K_a by Calculation (mGy/h)
Zr	Cu	8.64	50	10	6.0605	
				20	11.7126	10.90
Mo	Zr	17.5	80	10	27.7091	
				20	54.52	48.39
Sn	Ag	25.3	100	10	18.1072	16.95
				20	35.6880	
Nd	Ce	37.4	110	10	4.9672	4.89
				20	9.7437	
Er	Gd	49.1	120	10	5.3784	4.72
				20	10.4960	
W	Yb	59.3	170	10	6.0860	5.60
				15	9.0546	
Au	W	68.8	170	10	1.9144	1.79
				15	2.8697	
Pb	Au	75	200	10	5.1987	5.12
				15	7.7691	

ing radiations were less than 3% in this system. The air kerma rates were up to 54.52 mGy/h in Mo radiator. Though it may take long times to irradiate the personal dosemeters with the W radiator because of its low air kerma rate (1.91 mGy/h) but it dose not make a big problem to investigate the sensitivity change of the dosemeter with the energies.

An interchangeable radiator and filter system could be used such that the radiator, optimum high voltage and current are easily selected for a particular K fluorescent X-ray energy and air kerma rate. The established system offers a high beam intensity of monochromatic radiation from a few keV up to 75 keV with ease and convenience of operation. By this study the KAERI radiation calibration laboratory can calibrate the radiation instrument with the monochromatic radiations from ~ 8.6 keV (K_α of Zn) to 1,250 keV (^{60}Co), and particularly these K fluorescent X-ray beams will be used for the determination of energy responses of the personal dosemeters to compare with those of continuous X-ray energy distribution.

References

1. ICRU, *Determination of Dose Equivalents from External Radiation Sources - Part 3*, ICRU Report 47, Bethesda, MD(1992).
2. ICRP, *Data for Use in Protection Against External Radiation*, ICRP Publication 51(1987).
3. ICRP, *Conversion Coefficients for Use in Radiological Protection Against External Radiation*, ICRP Publication 74(1997).
4. ANSI, *American National Standard for Dosimetry - Personnel Dosimetry Performance Criteria for Testing*, ANSI N13.11(1993).
5. International Organization for Standardization, *X-Ray and Gamma Reference Radiation for Calibrating Dosemeters and Dose Ratemeters and for Determining Their Response as a Function of Photon Energy*, ISO 4037 Part1(1992).
6. E.Gillam and H.Heal, *Some Problems in the Analysis of Steels by X-Ray Fluorescence*, British J. of Appl. Phys., Vol. 3, 353-358(1952).
7. H.J.Beattie and R.M.Brissey, *Calibration Met hod for X-Ray Fluorescent Spectrometry*, Analytical Chem., Vol. 26, No. 6, 980-983(1954).
8. J. Sherman, *The Theoretical Derivation of Fluorescent X-Ray Intensities From Mixtures*, Spectrochimica Acta, Vol. 7, 283-306 (1955).
9. T.Shiraiwa and N.Fujino, *Theoretical Calculation of Fluorescent X-Ray Intensities inFluorescent X-Ray Spectrochemical Analysis*, Japanese J. of Appl. Phys., Vol.5, N0.10, 886-899(1966).
10. R.L.Kathren, F.L.Rising and H.V.Larson, *K-Fluorescence X-Rays: A Multi-Use Tool for Health Physics*, Health Phys., Vol. 21, 285-293 (1971).
11. J.L.Chartier, G.Portal, D.Roman and D.Duguay, *Production de Rayonnements Monoch-romatiques Intenses*, Nucl. Instru. Meth.,Vol. 100, 107-119(1972).
12. E.J.Hoffman and M.E.Phelps, *Production of Monoenergetic X-Rays from 8 to 87 keV*, Phys., Med. Biol., Vol. 19, No.1, 19-35(1974).
13. B.Kohnoura and K.Minami, *Establishment of Fluorescent X-Ray Irradiation Field for Calibrating Radiation Measuring Instruments*, 保健物理, Vol. 25, 147-154(1990).
14. R.A.Fox, C.D.Hooker abd J.C.McDonald, *A Method of Generating K-Fluorescent X-Rays*, American Nucl. Soc. Topical Meeting held in Richland, USA(1992).
15. H.H.Hsu, D.G.Vasilik and J.Chen, *An Optimal Target-Filter System for Electron Beam Generated X-Ray Spectra*, Nucl. Instru. Meth. in Phys. Res. A355, 641-644(1995).
16. W. J. Illes, *The Computation of Bremsstrahlung X-Ray Spectra Over an Energy Range 15 keV to 300 keV*, NRPB-R204(1987).
17. J.L Kim, B.W.Kim, S.Y.Chang and J.K.Lee, *Calculations of ISO Narrow and ANSI X-RaySpectra, Their Average Energies and Conversion Coefficients*, Korea Ass. for Ra-

dia. Prot., Vol. 20, No. 2, 129-136(1995).
18. 장시영 외, *방사선 방어 및 측정기술개발, 원자력연구개발 중장기과제보고서*, KAERI/RR--1739/96(1997).
19. J.L Kim, B.W.Kim, S.Y.Chang and J.K.Lee, *Establishment of ANSI N13.11 X-Ray Radiation Fields for Personal Dosimetry Performance Test by Computation and Experiment*, Environ. Health Pers., Vol. 105, Supp. 6, 1417-1422(1997).
20. J.L.Chartier, D.Roman and A.Bazoge, *Problems of Exposure Measurement with Extended Source; Case of X-Ray Fluorescent*, Nucl. Instru.. Meth., Vol. 119, 427-444(1974).